

Differentiating Between Modified Gravity Theories in the Solar System

Ali Mozaffari¹

¹ *Theoretical Physics Group, Imperial College, London, SW7 2BZ**
(Dated: June 9, 2018)

Building on previous work, we re-examine the possibility of testing MOdified Newtonian Dynamics near the saddle points of gravitational potentials in the Solar System, through an extension of the forthcoming LISA Pathfinder mission. We extend present analysis to include quasi-linear formulations of these theories, resulting from fully relativistic modified gravity theories. Using similar quantitative and qualitative tools, we demonstrate that in general, both the instrumental response and typical Signal to Noise Ratios for such a test will be different. Finally we investigate constraints from a negative result and parameterised free functions.

PACS numbers: 04.50.Kd, 04.80.Cc

1. Introduction

The standard model of cosmology is composed of General Relativity and Λ CDM which has had great success in matching large scale observations in astronomy and cosmology. However attempts to date to directly detect candidate dark matter particles have been at best unclear and at worst fruitless. Over the past few decades, attempts to reconcile anomalous observations of galactic dynamics without resorting to dark matter have been the driving forces behind modified gravity theories. These have centred around a prescription for a modified force law [1], which reduce to Newtonian dynamics at “large” accelerations and modified dynamics at “small” accelerations (large and small here are relative to the Milgrom characteristic acceleration taken here as $a_0 \approx 10^{-10} \text{ ms}^{-2}$). In doing so, the observed flattening of galaxy rotation curves and the empirical Tully-Fisher relation can both be satisfied [2]. Recent work on an experimental observation of theories with a preferred acceleration scale [3, 4, 5] suggest that anomalously large tidal stresses should be present around the gravitational saddle points (SP) scattered throughout the Solar System. The proposed LISA Pathfinder (LPF) mission [6] could be capable of serving as an accelerometer of unprecedented accuracy. The instrument, essentially, consists of two test masses, orientated such that they are in a free fall, with a laser interferometer between them. In this way, it is possible to measure the differential acceleration between the two bodies and hence infer the tidal stresses (by factoring the inter mass spacing). With such an instrument, we suggest it could be possible to observe the onset of MONDian behaviour (rather than at the scales present at galaxies, where MONDian behaviour will dominate the dynamics) in the low acceleration regime around these SP. The purpose of this paper is extend previous analyses done for the modified gravity saddle point science case, based upon a scenario where

an LPF mission extension is granted. This would involve redirecting the spacecraft from its location parked at Lagrange point L1 to a saddle of the Sun-Earth-Moon system [7] once its nominal mission is completed. Previous analysis have considered non-linear theories with modified Poisson equations, which naturally give rise to modified gravity behaviour (as seen most clearly in [8]). A review of the different non-relativistic limits of preferred acceleration scale theories [5] categorised these as types I, II and III (we summarise these briefly in Appendix A). In this work, we examine type II theories, where the dynamics are governed by a physical potential Φ , composed of $\Phi = \Phi_N + \phi$, with the usual

$$\nabla^2 \Phi_N = 4\pi G\rho \quad (1)$$

The field ϕ is ruled by a driven linear Poisson equation

$$\nabla^2 \phi = \frac{k}{4\pi} \nabla \cdot (\nu(w) \nabla \Phi_N) \quad (2)$$

where the argument of free function ν is given by

$$w = \left(\frac{k}{4\pi} \right)^2 \frac{|\nabla \Phi_N|}{a_0} \quad (3)$$

and we require that $\nu \sim 1/\sqrt{w}$ for $w \ll 1$ and that $\nu \rightarrow \text{constant}$ when $w \gg 1$. Consider now just writing

$$\nabla^2 \Phi = \nabla \cdot (\hat{\nu}(w) \nabla \Phi_N) \quad (4)$$

where $\hat{\nu} = 1 + \frac{\kappa}{4\pi} \nu$. We can divide our theories into two distinct subclasses, where crucially

$$\nu \rightarrow 0 \quad \text{IIA} \quad (5)$$

$$\nu \rightarrow 1 \quad \text{IIB} \quad (6)$$

Type IIB theories in the large acceleration regime have $G_{ren} = G(1 + \kappa/4\pi)$, due to the scalar field mimicking a rescaled Newtonian potential $\phi \rightarrow \frac{\kappa}{4\pi} \Phi_N$. In IIA theories, it can be argued we need only a single physical potential Φ and Newtonian field Φ_N plays only an auxiliary role (and so κ need not appear at all) - meaning there is no G renormalisation. As pointed out in [5], the

*Electronic address: ali.mozaffari05@imperial.ac.uk

effect of which is that the triggering of MONDian effects would happen at $a_{trig} = a_0$ (at a distance of $r \sim 2.2m$ from the saddle). With such a tiny bubble, these theories would escape the net of an LPF test, at least for the Earth-Sun system. With this in mind, we will stick to type IIB theories here, the case for testing other types of MONDian theory have been considered separately [5, 9]. Similarly, we stress that it is important that we consider formulations wedded to fully relativistic theories (rather than just a scalar Lagrangian theory like AQUAL [10]), even though we are not directly testing these full theories themselves. Their cosmologies however, do provide the necessary constraints on the gravitational constant G , the *bare* value of G appears in the Friedman equations and so from BBN constraints can be fixed. As we will see, this issue is not a trivial one in modified gravity theories. Deriving the full field equations and taking the weak field limit as necessary allows us to find the modified Poisson equations for these theories consistently. To this end, we will consider a theory arising from BiMOND [11]. Additionally readers should consider the cosmologies of these theories, as suggested in [12].

The structure of this paper is as follows, we firstly consider analytical and numerical solutions from solving this theory around the Earth-Sun SP. Next we move onto consider the integrated signal to noise ratio (SNR) as a measure of how sensitive the LPF instruments will be, the main results of which are contained in Figures 3 and 4. A look at converting a null signal into a constraint on the parameter space of our theories is the subject of Section 2 - seeing whether we could differentiate between different modified gravity theories. Finally Section 4 looks at parameterised approaches to these theories and looks to the future. We leave detailed derivations and computational methods to the appendices.

2. Solutions, Tidal Stresses and Signal to Noise Ratios

In this analysis, we will make use of both analytical and numerical results. We suggest using a free function ν of the form

$$\nu = \left(1 + \frac{1}{w^2}\right)^{1/4} \quad (7)$$

We outline in Appendix B some reasons for this choice and with it we solve Equation ?? around the SP (recalling we are free of sources),

$$\nabla^2 \phi = \frac{\kappa}{4\pi} \nabla \cdot (\nu \nabla \Phi_N) = \frac{\kappa}{4\pi} \left(\underbrace{\nu \nabla^2 \Phi_N}_{=0|_{SP}} + \nabla \nu \cdot \nabla \Phi_N \right)$$

We can approximate the Newtonian near to the SP with a linear profile, which in spherical coordinates takes the

form,

$$\begin{aligned} \mathbf{F}_N &= -\nabla \Phi_N = Ar\mathbf{N} = Ar(N_r \mathbf{e}_r + N_\psi \mathbf{e}_\psi) \\ N_r &= \frac{1}{4}(1 + 3 \cos 2\psi) \\ N_\psi &= -\frac{3}{4} \sin 2\psi \end{aligned} \quad (8)$$

Using this form of the Newtonian field as our source, we proceed to solving the resulting system of equations. Recall that the we have both a deep MONDian (DM) regime, close to the saddle where $w \ll 1$ and an quasi-Newtonian (QN) regime further out, where $w \gg 1$. Separating these will be a boundary which using the linearised Newtonian we can find,

$$w = \left(\frac{\kappa}{4\pi}\right)^2 \frac{Ar|\mathbf{N}|}{a_0} = 1 \quad (9)$$

$$r^2 \left(\cos^2 \psi + \frac{1}{4} \sin^2 \psi \right) = r_0^2 = \left(\frac{16\pi^2 a_0}{\kappa^2 A} \right)^2 \quad (10)$$

As such we find an ellipsoidal (or bubble shaped) boundary, with semi-major axis which we denote r_0 . Solving the system, for the particular choice of $\nu(w)$, we have for the inner bubble,

$$\begin{aligned} -\nabla \phi &= \frac{4\pi a_0}{\kappa} \left(\frac{r}{r_0}\right)^{0.5} (F_r \mathbf{e}_r + F_\psi \mathbf{e}_\psi) \\ F_r &\approx 0.0354 + 0.2829 \cos 2\psi - 0.0162 \cos 4\psi \\ F_\psi &\approx -0.3772 \sin 2\psi - 0.0432 \sin 4\psi \end{aligned} \quad (11)$$

and similarly for the outer bubble

$$\begin{aligned} -\nabla \phi &= \frac{4\pi a_0}{\kappa} \left[\frac{r_0}{r} (F_r \mathbf{e}_r + F_\psi \mathbf{e}_\psi) + \frac{r}{r_0} \mathbf{N} \right] \\ F_r &= 1 \\ F_\psi &\approx -0.5752 \sin 2\psi + 0.4652 \sin 4\psi \end{aligned} \quad (12)$$

(The full calculational details are left to Appendix B). Now we can consider numerical solutions, using a relaxation code to solve (2) on an adaptive lattice. Such a code was first employed to study these theories in [4] and subsequently adapted for more general free functions in [8]. In Appendix C, we detail the modifications required for this work. Consider the Earth-Sun saddle, using a 257^3 lattice of physical size 10^4 km with a typical central resolution of ~ 2.6 km. Running the code delivers us predictions for the modified forces close to the saddle, which as Figure 1 shows are a good match to analytical solutions in their respective domain and provide the appropriate interpolation in the intermediate region. Next consider that LPF is sensitive to differential acceleration, from which we can infer the tidal stresses of our signal. Note also that the ϕ field produces both a MONDian effective field and a rescaled Newtonian component. Taking these into account, the observable tidal stress will be of the form

$$S_{ij} = -\frac{\partial^2 \phi}{\partial x_i \partial x_j} + \frac{k}{4\pi} \frac{\partial^2 \Phi^N}{\partial x_i \partial x_j} \quad (13)$$

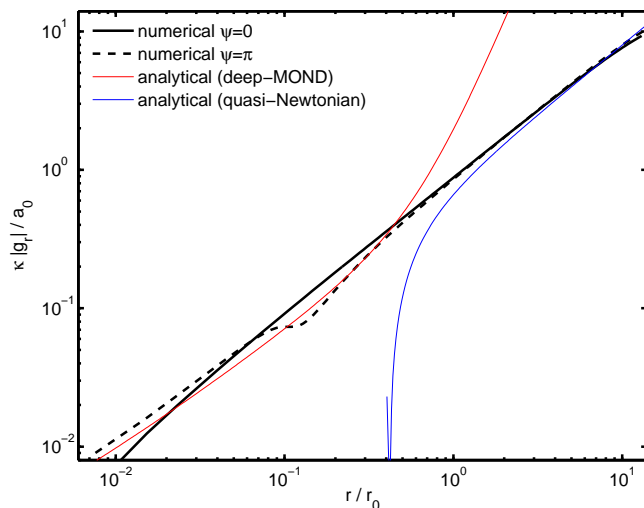


FIG. 1: A comparison between the numerical and analytical results for a component of $\mathbf{g} = -\nabla\phi$ around the Earth-Sun saddle.

It is important that we know both field components to the same degree of accuracy or systematic errors can crop up due to the imperfect subtraction of the Newtonian field. Using the techniques of noise matched filtering from gravitational wave searches [13], we can compute the Signal to Noise Ratios (SNR) of these anomalous tidal stresses with LPF. The basic idea laid is to correlate a time series $x(t)$ with an optimized template designed to provide maximal SNR, given the signal shape $h(t)$ and the noise properties of the instrument. Whilst the specifics of the instrument noise won't be known properly until the satellite is *in situ*, there exist nominal requirements that it must meet [14], as well as best estimates for the noise signal waveform. In our setup, we align the line joining the Sun-Earth as our x axis, such that we have trajectories of the form

$$h(t) = S_{yy}(vt, b, 0) \quad (14)$$

where v is the velocity of the spacecraft, b is the impact parameter and $t = 0$ corresponds to the point of closest saddle approach. In a more general setup, for an approximately constant velocity \mathbf{v} , a closest approach vector \mathbf{b} , and with the masses aligned along unit vector \mathbf{n} ,

$$h(t) = n^i n^j S_{ij}(\mathbf{b} + \mathbf{v}t) \quad (15)$$

The maximal SNR, realised by correlating the optimal template with the noise, is found to be

$$\rho_{\text{opt}} = 2 \left[\int_0^\infty df \frac{|\tilde{h}(f)|^2}{S_h(f)} \right]^{1/2} \quad (16)$$

where $\tilde{h}(f)$ is the Fourier transformed signal waveform and $S_h(f)$ is the noise waveform in Fourier space. To

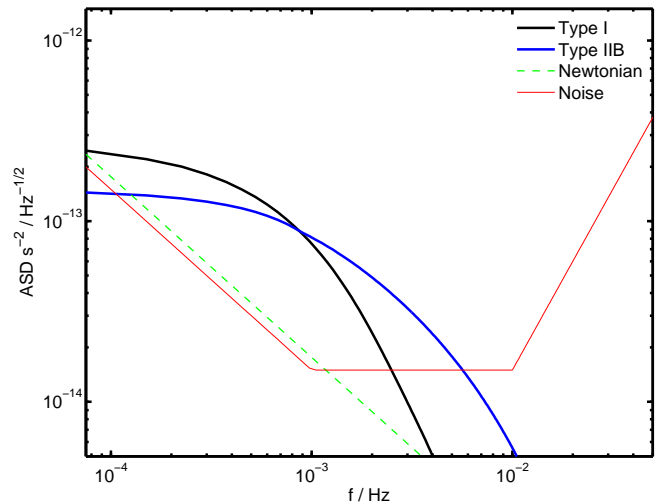


FIG. 2: ASD plot of the MONDian and rescaled Newtonian signals, along with the noise profile. Using the parameters $b = 50\text{km}$ fly-by and $v = 1.5\text{ ms}^{-1}$, we compare between type I and IIB theories, finding in this scenario SNRs of 28 and 35, respectively.

make this analysis concrete, consider a flyby at $b = 50\text{km}$. We plot the noise and signal, terms of amplitude spectral density (ASD), which is simply square root of power spectrum, in Figure 2. As we see, there is ample signal compared to idealised noise (here with baseline $1.5 \times 10^{-13}\text{ s}^{-2}/\sqrt{\text{Hz}}$). This scenario gives an SNR of 35 and for comparison a type I signal is presented giving an SNR of 28 - note the differences in the behaviour at low and high frequencies. The larger SNR here stems from the Poisson equation being linear in $\nabla\phi$ and hence there are no associated curl forces (which generally exist in non-linear theories). These will produce a softening of the tidal stress divergence, since this is not present here, we find a larger signal. We produce in Figure 3 contours for typical SNRs produced at various impact parameters and baseline noises, as well as present a comparison of contours from different theories - observing that type IIB beats type I on SNR. As Figure 2 shows, the position of the signal in fourier space is exactly where noise is lowest. This highlights an uncanny coincidence, given that the accelerometer aboard LPF has a non-white noise profile, dipping in the region of the mHz (on the rough time scale of minutes). The motivation for such a design lies in the gravitational wave signals to be targeted by LISA - it just happens that the MONDian bubbles of anomalous tidal stresses around the Earth-Sun-Moon saddles are of length scale $\sim 10^3\text{ km}$ and free-falling bodies around this region have a typical speed of $\sim 1\text{ km s}^{-1}$. Put together, this suggests the time scale for crossing a MONDian bubble would be on the order of minutes - right where the instrument performance is optimal.

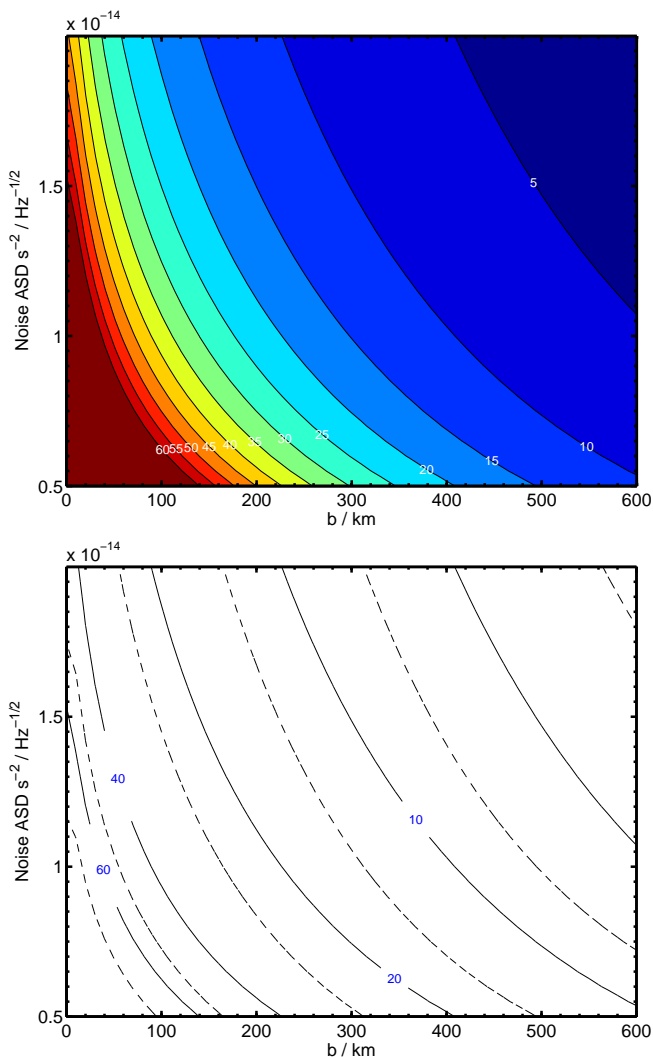


FIG. 3: **Top panel**, SNR contours for various impact parameters and baseline ASD noise, for $v = 1.5 \text{ km s}^{-1}$. Calamitous assumptions would still lead to SNR in excess of 5. More optimistic ones (b around 50km or less, noise half way up the scale) would lead to SNRs easily around 55. **Bottom panel**, a comparison of SNR contour lines between type I and IIB theories. The solid lines are the typical SNR to be obtained in IIB theories and the dashed lines to their immediate left the corresponding type I - as we see IIB beats I.

3. Designer ν functions

It is very easy to construct free functions which mimic parameterised galactic $\tilde{\mu}$ functions [15], for instance

$$\nu = \frac{w^{-1/2}}{1 + \frac{4\pi\alpha}{\kappa} w^{n-1/2}} \quad (17)$$

giving the usual $\nu \rightarrow 1/\sqrt{w}$ in the DM regime but moving to a different power law, $\nu \sim 1/w^n$ (tunable by the value of α) for larger accelerations. We can attempt the exercise of designing a free function, based on a null result

(taking an upper bound from a SNR = 1 result) at some acceleration. We can then convert this into a restriction on the ν parameter space - clearly the SP bubble clearly will have to shrink. We start by fixing the asymptotica, the astrophysical regime gives us $\nu \approx 1/\sqrt{w}$ for $F_N \leq a_0$. Far from the SP, we will have the $\nu \approx 1$ regime, but in the intermediate regime between the two (which we will be probing), let's suggest a model such as:

$$\nu \approx 1/\sqrt{w} \quad \text{for} \quad w < \left(\frac{k}{4\pi}\right)^2 \quad (18)$$

$$\nu \approx \left(\frac{w^{trig}}{w}\right)^n \quad \text{for} \quad \left(\frac{k}{4\pi}\right)^2 < w < w^{trig} \quad (19)$$

$$\nu \approx 1 \quad \text{for} \quad w > w^{trig} \quad (20)$$

where the point when non-Newtonian behaviour in ϕ is triggered can be interchangeably pinpointed by:

$$w^{trig} = \left(\frac{\kappa}{4\pi}\right)^{2-\frac{1}{n}} \quad (21)$$

$$a_\phi^{trig} = a_0 \left(\frac{\kappa}{4\pi}\right)^{1-\frac{1}{n}} \quad (22)$$

$$a_N^{trig} = a_0 \left(\frac{\kappa}{4\pi}\right)^{-\frac{1}{n}} \quad (23)$$

We still have that when $a_N < a_0$, the field ϕ dominates Φ_N - as per our requirements. However now the intermediate region where ϕ hasn't yet dominated but is already non-Newtonian is in a narrower band of accelerations $a_0 < a_N < a_N^{trig}$. As a result, the MOND bubble shrinks in this model according to

$$r_0 \approx 383 \left(\frac{\kappa}{4\pi}\right)^{\frac{2n-1}{n}} \text{ km} \quad (24)$$

This result shows that for a given null measurement up to some acceleration a_N^{trig} , using this general argument, our constraints between type I and IIB theories will be different. In this case, the bubble size would be expected to shrink more than in the type I case (where the exponent is just $\frac{n-1}{n}$ [5]), given the sharper divergence in the tidal stress (and so larger signal) and this is exactly what (24) suggests. Thus our naive expectation that the bubble would be smaller, given the stronger signed expected, compared to type I theories turns out to be true. One issue that we come up against here is that because of there are many varying transients from $\nu \rightarrow 1$, making a model dependent statement is beyond our reach - quite simply because a null result only lets us probe the regime of $b \gg r_0(n)$. Performing an order of magnitude argument however is possible using a designer function,

$$\nu(w) = 1 + \left(\frac{w^{trig}}{w}\right)^n \quad (25)$$

Assuming spherical symmetry

$$\mathbf{F}_\phi = \frac{k}{4\pi} \nu \mathbf{F}_N \quad (26)$$

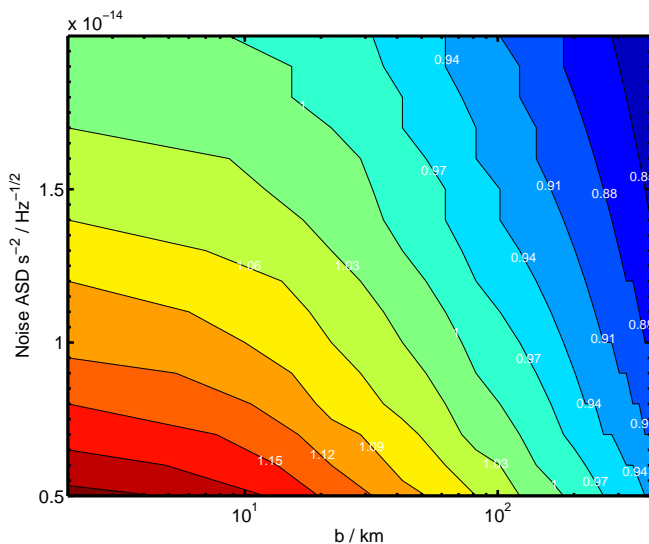


FIG. 4: Contours of the power n needed to obtain SNR = 1 for different impact parameters and noise levels, upto $b = 400$ km using our designer free function.

breaking this up into a background contribution and a modified part

$$\mathbf{F}_\phi = {}^0\mathbf{F}_\phi + \delta\mathbf{F}_\phi \quad (27)$$

where ${}^0\mathbf{F}_\phi = \frac{\kappa}{4\pi}\mathbf{F}_N$. Substituting in and solving gives

$$\delta\mathbf{F}_\phi = \frac{k}{4\pi}(\nu - 1)\mathbf{F}_N \simeq \left(\frac{a_0}{|\mathbf{F}_N|}\right)^n \mathbf{F}_N \quad (28)$$

from which the tidal stresses can be inferred. Figure 4 shows the resulting values of n required for a SNR = 1 result. As we see, the dynamics here are somewhat different which opens up the future possibility of letting us differentiate between type I and IIB theories. A result in one theory could be considered “unnatural” but could possibly be viable in another.

4. Parameterised Free Functions

Other questions to be asked include what inferences can we make from data if LPF detects anything (after ruling out systematics and noise). Is it possible to pick out particular features of our free functions? Would there be a way to potential discriminate between different types of theory? Here we seek to address some of these briefly. Firstly, lets develop a parameterised $\nu(w)$, which will act as a prototype for further discussions,

$$\nu = \left(\frac{1 + w^b}{w^b}\right)^{a/b} \quad (29)$$

notice that in the requisite limits

$$w \ll 1, \quad \nu \simeq \frac{1}{w^a} + \dots \quad (30)$$

$$w \gg 1, \quad \nu \simeq 1 + \frac{a}{b} \frac{1}{w^b} + \dots \quad (31)$$

This reduces back to MOND for the case of $a = \frac{1}{2}$ and $b \geq 1$, but otherwise opens up the parameter space. Equation type II Laplacian has the form

$$\begin{aligned} \nabla^2\phi &= \frac{4\pi a_0}{\kappa} \frac{a r_0^{b-1}}{r^b N^b} \left(N_r + \frac{\partial N}{\partial \psi} \frac{N_\psi}{N}\right) \left(1 + \left(\frac{r_0}{rN}\right)^b\right)^{a/b-1} \\ &\simeq C_1 r^{c-2} S_c(\psi) + \dots \end{aligned} \quad (32)$$

An ansatz for the leading order contribution takes the form

$$\phi = C_1 r^c F(\psi) \quad (33)$$

with the profile function $F(\psi)$ satisfying the ODE

$$c(c+1)F + F' \cot \psi + F'' = S_c(\psi) \quad (34)$$

Note this satisfies the equations $b \neq 2$ and we will consider the $b = 2$ case separately later. The constant and source terms are given by

$$C_1 = a \frac{4\pi a_0}{\kappa} r_0^{c-3} \quad (35)$$

$$S_c(\psi) = \frac{1}{N^{c-2}} \left(N_r + \frac{\partial N}{\partial \psi} \frac{N_\psi}{N}\right) \quad (36)$$

such that in each regime

$$c = 2 - a \quad w \ll 1 \quad (37)$$

$$c = 2 - b \quad w \gg 1 \quad (38)$$

With these in mind, we can solve the inhomogenous ODE, as before, to find the variation in profile functions for different a, b . To make a connection with other modified force laws [8], consider under spherical symmetry:

$$\begin{aligned} \left(\frac{\kappa}{4\pi} \frac{F_\phi}{a_0}\right)^n F_\phi &= \frac{\kappa}{4\pi} F_N \Rightarrow F_\phi = \left(\frac{\kappa}{4\pi}\right)^{\frac{1-n}{1+n}} F_N^{\frac{1}{1+n}} a_0^{\frac{n}{1+n}} \\ F_\phi &= \left(\left(\frac{\kappa}{4\pi}\right)^2 \frac{F_N}{a_0}\right)^{-a} \frac{\kappa}{4\pi} F_N = \left(\frac{\kappa}{4\pi}\right)^{1-2a} F_N^{1-a} a_0^a \end{aligned} \quad (39)$$

and so let us, without loss of generality, parameterise

$$a \rightarrow \frac{n}{n+1} \quad (40)$$

This means the choice of $n = 1 \Leftrightarrow a = 1/2$ gives the required force law $F_\phi = \sqrt{F_N a_0}$ and some $n > 1$ will parameterise deviations from it. We illustrate different choices of b, n in Figure 5. The take home message from this analysis is that in the strongly modified regime of the inner SP bubble, there is little variance between the

potentials - the main difference is from the radial exponent. This means one can expect the magnitude of any resulting anomalous tidal stresses to be different rather than the shape of the time series. This has an impact on the noise matched filtering techniques of Section 2, as the space of inner bubble templates can effectively be significantly reduced. With this generalised approach, consider the tidal stresses S_{yy} computed by employing a change of variables

$$S_{yy} = C_2 r^{c-2} ((c-2) \cos 2\psi - c) cF - 2 \cos \psi (2(c-1) \sin \psi F' + \cos \psi F'') \quad (41)$$

where $C_2 = C_1/2$. Although slightly complicated, this expression demonstrates that in the regime where the linear Newtonian 8 can be applied, there is a neat separation of variables between radial and azimuthal functions. Notice that in all these models, the stresses will be divergent since $c < 2, \forall a, b > 0$. For the $b = 2$ case,

$$\phi = \frac{4\pi a_0}{\kappa} \left(r_0 \ln \left(\frac{r}{r_0} \right) + H(\psi) \right) \quad (42)$$

$$S_{yy} = -\frac{4\pi a_0}{\kappa r^2} (r_0 \cos 2\psi - \sin 2\psi F' + \cos^2 \psi F'') \quad (43)$$

where $H(\psi)$ is a function solved by the second order ODE (34) sourced by (36). The main reasoning behind the invariance of profile functions in the low acceleration regime and the Smörgåsbord of solutions in the other stems from the behaviour of the source term

$$\lim_{\psi \rightarrow \pi/2} S_c = -2^{c-3} \quad (44)$$

For $0 < a < 1$, S_c remains relatively unchanged compared to $b > 0$ where S_c becomes increasingly singular at $\psi = \pi/2$ for increasing b . Observe that $S_{yy} \sim r^{-\#}$ where $\nu \rightarrow w^\#, w \ll 1$ or $\nu \rightarrow 1 - \frac{C}{w^\#} + \dots, w \gg 1$ whereas in the type I case [8], S_{yy} was found to scale much more conservatively in the DM regime.

5. Conclusions

Our investigations have shown how a LPF saddle flyby could either detect modified gravitational behaviour to a high SNR or place stringent constraints on it. With an appropriate noise model, SNRs ≥ 35 could be expected missing the saddle by 50km or less (a larger figure than would be expected from type I theories). The question then arises as to how generic this conclusion is, or conversely, should a negative result be found what can be said about these theories. Predictions for what happens inside the bubble are found to be model independent, the tidal stress anomalies outside the bubble however do depend on the transient from the modified into the Newtonian regime, with a model dependent fall-off. Thus for impact parameters smaller than r_0 the predicted SNRs

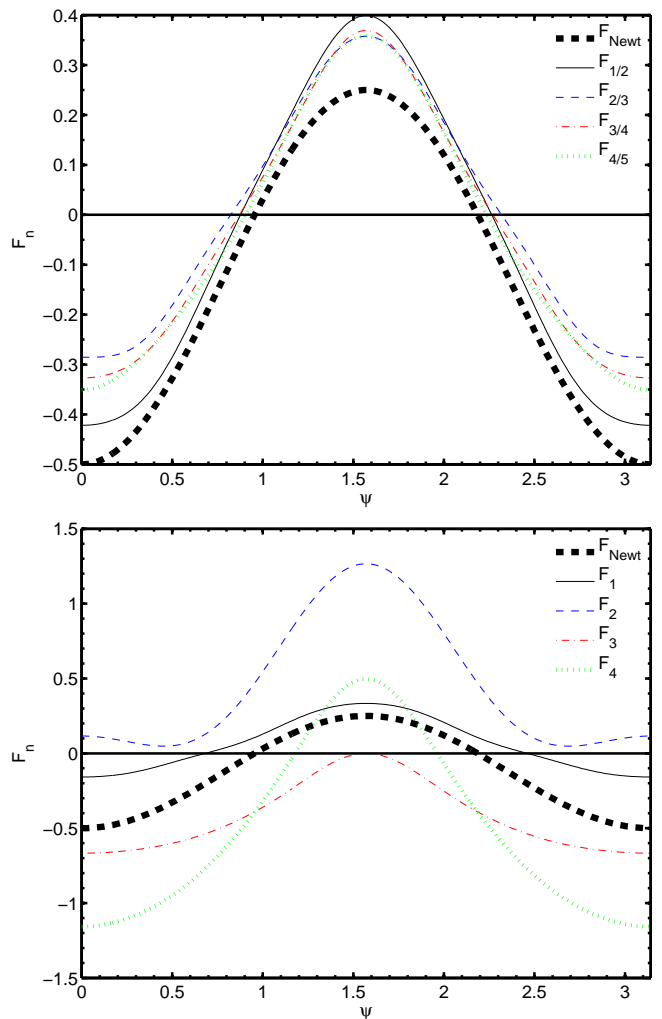


FIG. 5: The angular profile functions F for the inner (**top panel**) and outer (**bottom panel**) bubble regions, alongside the linear Newtonian potential profile F_{Newt} . The values of a, b are used to label each function. The results clearly show the relative invariance of the inner bubble potential profile functions compared to the significant differences for the outer bubble.

are robust and do not change substantially - the currently expected case is $b \leq 10$ km (with $r_0 \sim 383$ km). A way therefore for such theories to wriggle out of a negative LPF result would be to change the bubble size. This could be accomplished with a “designer” function - giving the free function two scales and two power-laws before reaching the rescaled Newtonian regime. Furthermore the effects inside the bubble are different from type I predictions, but generically stronger. This stems from type II theories lack of curl field, a feature which appears to soften out the anomalous stresses. This results generically in larger SNRs between type I and IIB theories. As we see applying the same arguments between the two theories results in different constraints and the bubble size generically being smaller here compared to type I for a

null result. By considering a generalised approach to free functions, we find inner and outer bubble solutions and considered the scaling of the tidal stress with parameters extracted from the free functions. The main result being that in the DM regime, our angular profile functions become relatively invariant between models, making the prospect of extracting features of ν from potential data interesting - the main contribution being the radial parameter and its associated exponent. The divergence of the tidal stresses scale much quicker for a given $\nu(a, b)$ compared to the corresponding $\mu(a, b)$ models of type I theories. These models suggest that tying a result to either type I or IIB theories is in principle viable - differentiating between the two theories is a realistic prospect, our imagination is only limited to the theories we develop.

Acknowledgments

The author would like to thank João Magueijo, Tim Clifton, Johannes Noller and Dan Thomas for useful discussions and suggestions. The author thanks the STFC, Department of Physics and Centre for Co-Curricular Studies, Imperial College for financial support during the various stages of this work. Numerical work was carried out on the COSMOS supercomputer, which is supported by STFC, HEFCE and SGI.

Appendix A: Classifying MONDian theories

Our job is to approach theories where such modified behaviour is present and see if they represent good prospects for detection. Their complexity and differences arise from the requirement that they should explain relativistic phenomena (such as lensing and structure formation) without appealing to dark matter, whilst in the non-relativistic regime have some Newtonian and other modified limit. The manner in which such effects are manifest may however vary widely and there have been many previous studies as to the phenomenology of these ideas, particularly in this non-relativistic regime [5, 9, 11, 16, 17]. We will briefly outline some of these here, with the caveat that this list is neither exhaustive, nor represents the final story on gravity theories at the time of writing and for a more in depth look at gravity theories, we point the reader towards [18].

- **Type I:** Here the total potential acting on non-relativistic particles is given by the sum of the usual Newtonian potential Φ_N and a fifth force field, ϕ :

$$\Phi = \Xi\Phi_N + \phi \quad (\text{A1})$$

where Ξ is some constant usually set to unity and the Newtonian potential satisfies the usual Poisson equation $\nabla^2\Phi_N = 4\pi G\rho$, and the field ϕ is governed by:

$$\nabla \cdot (\mu(z)\nabla\phi) = \kappa G\rho \quad (\text{A2})$$

The argument of $\mu(z)$ is given by

$$z = \frac{\kappa}{4\pi} \frac{|\nabla\phi|}{a_0} \quad (\text{A3})$$

where κ is a dimensionless coupling constant. μ is a free function, typically chosen limits of the theory are $\mu \rightarrow 1$ when $z \gg 1$ and $\mu \simeq z$ for $z \ll 1$. The effect of these fields is twofold, in the large z regime, $\phi \rightarrow \frac{\kappa}{4\pi}\Phi_N$ mimicking the Newtonian, this makes the physical potential have the form

$$\nabla\Phi \rightarrow \left(\Xi + \frac{\kappa}{4\pi}\right)\nabla\Phi_N \quad (\text{A4})$$

or equivalently the form of Newton's constant is altered

$$G_{ren} \rightarrow \left(\Xi + \frac{\kappa}{4\pi}\right)G_N \quad (\text{A5})$$

Cosmology sets bounds on the variation of G , from BBN and effects in the CMB [19, 20].

Additionally these two fields mean that the Newtonian behaviour is always present in the non-relativistic regime and non-linear behaviour in ϕ gets triggered at a certain acceleration

$$a_{trig} = \left(\frac{4\pi}{\kappa}\right)^2 a_0 \quad (\text{A6})$$

The field however remains sub-dominant until $a_N = a_0$ and this is when fully modified behaviour is seen (in the galactic regime). It is this onset of non-linearity that we hope to probe with LPF.

- **Type II:** These are similar in set-up to type I, with $\Phi = \Phi_N + \phi$ and ϕ governed by a driven linear Poisson equation:

$$\nabla^2\phi = \frac{\kappa}{4\pi}\nabla \cdot (\nu(w)\nabla\Phi_N) \quad (\text{A7})$$

The argument of ν is given by

$$w = \left(\frac{\kappa}{4\pi}\right)^2 \frac{|\nabla\Phi_N|}{a_0} \quad (\text{A8})$$

Once again ν is a free function and typically we give it the form $\nu \simeq 1/\sqrt{w}$ for $w \ll 1$ and $\nu \rightarrow \text{constant}$ for $w \gg 1$.

We divide this up in the subtypes of **IIA** or **IIB** with qualitatively very different implications, which can we seen more clearly if we return to using the physical potential form

$$\nabla^2\Phi = \nabla \cdot (\dot{\nu}\nabla\Phi_N) \quad (\text{A9})$$

$$\dot{\nu} = 1 + \left(\frac{\kappa}{4\pi}\right)\nu \quad (\text{A10})$$

Consider in the large w regime:

- In type **IIA**, $\nu \rightarrow 0$ which implies no G renormalisation occurs and $a_{\text{trig}} = a_0$. The whole theory in fact hinges on Φ , all other fields are considered auxiliary.
- In type **IIB**, $\nu \rightarrow 1$ means a trigger acceleration similar to type **I**.

- **Type III:** Crucially, here non-relativistic particles are sensitive to a single field Φ , satisfying a non-linear Poisson equation:

$$\nabla \cdot (\tilde{\mu}(x) \nabla \Phi) = 4\pi G \rho \quad (\text{A11})$$

where the argument of $\tilde{\mu}$ is

$$x = \frac{|\nabla \Phi|}{a_0} \quad (\text{A12})$$

so that $\tilde{\mu} \rightarrow 1$ when $x \gg 1$ and $\tilde{\mu} \sim x$ for $x \ll 1$. Again no renormalisation of G and a trigger acceleration $a_{\text{trig}} = a_0$

As the trigger acceleration sets the scale of the SP bubble, using the current estimates for our parameters ($\kappa = 0.03, a_0 = 10^{-10} \text{ ms}^{-1}$) we find these to be

$$\begin{aligned} a_{\text{trig}} &= \left(\frac{4\pi}{\kappa}\right)^2 a_0 \simeq 10^{-5} \text{ ms}^{-2} \Rightarrow r_0 \sim 383 \text{ km} \\ a_{\text{trig}} &= a_0 = 10^{-10} \text{ ms}^{-2} \Rightarrow r_0 \sim 2.2 \text{ m} \end{aligned} \quad (\text{A13})$$

These distinctions group together types **I** and **IIB** as the best candidates for detection with LPF; types **IIA** and **III** would easily escape any negative result.

An important distinction here stems from the fact that we have a curl term (often called a magnetic field) in type **I** and **III** theories. This is easiest seen when one attempts to linearize the non-linear Poisson equations present by introducing an auxiliary vector field (e.g. $\mu \nabla \phi$ for type **I** theories) - such a field has non-zero curl. The same is not true for type **II** theories, being already linear in ϕ and driven by a function of the Newtonian field, $\nu \nabla \Phi_N$, (a quantity which has a curl). This turns out to have a significant quantitative effect upon the magnitude of the saddle tidal stresses, as the magnetic field is known to soften the anomalous tidal stresses around the saddle points in type **I** theories.

Appendix B: Analytical Arguments

Our plan will be to consider functions similar to those investigated for type **I** theories and so easily compare between the two. We start with the idea that *under the assumption of spherical symmetry*

$$\begin{aligned} \nabla \cdot (\mu \mathbf{F}_\phi) &= \frac{\kappa}{4\pi} \nabla \cdot \mathbf{F}_N \Rightarrow \mu \mathbf{F}_\phi = \frac{\kappa}{4\pi} \mathbf{F}_N \\ \nabla \cdot \mathbf{F}_\phi &= \frac{\kappa}{4\pi} \nabla \cdot (\nu \mathbf{F}_N) \Rightarrow \mathbf{F}_\phi = \frac{\kappa}{4\pi} \nu \mathbf{F}_N \end{aligned} \quad (\text{B1})$$

with the natural comparison between

$$\mu(z) \longleftrightarrow \frac{1}{\nu(w)}$$

We will be inspired by the form of the type **I** free function μ considered previously [3, 4, 8], which satisfied

$$\frac{\mu}{\sqrt{1-\mu^4}} = z \quad (\text{B2})$$

where $z = \frac{\kappa}{4\pi} \frac{|\nabla \phi|}{a_0}$. In the $z \gg 1$ limit,

$$\mu \simeq 1 - \frac{1}{4z^2} + \dots \quad (\text{B3})$$

which suggests in the analogous $w \gg 1$ limit, we need a function satisfying

$$\nu \simeq 1 + \frac{1}{4w^2} + \dots \quad (\text{B4})$$

Using the definition of z , under spherical symmetry

$$z = \frac{\kappa}{4\pi} \frac{|\nabla \phi|}{a_0} = \nu \left(\frac{\kappa}{4\pi}\right)^2 \frac{|\nabla \Phi_N|}{a_0} = \nu w \quad (\text{B5})$$

$$\frac{\mu}{\sqrt{1-\mu^4}} = \frac{1/\nu}{\sqrt{1+1/\nu^4}} = \nu w \quad (\text{B6})$$

which we can solve to find

$$\nu = \left(1 + \frac{1}{w^2}\right)^{1/4} \quad (\text{B7})$$

and note in the quasi Newtonian regime, this mimics the behaviour of (B4). Whilst we stress this derivation is only strictly valid for spherical symmetry, it remains a good starting point for comparison between these theories. Next we expand the Poisson equation

$$\nabla^2 \phi = \frac{\kappa}{4\pi} \nabla \cdot (\nu \nabla \Phi_N) = \frac{\kappa}{4\pi} \left(\underbrace{\nu \nabla^2 \Phi_N}_{=0|_{SP}} + \nabla \nu \cdot \nabla \Phi_N \right)$$

and then use the linear Newtonian approximation,

$$\begin{aligned} \mathbf{F}_N &= -\nabla \Phi_N = Ar\mathbf{N} = Ar(N_r \mathbf{e}_r + N_\psi \mathbf{e}_\psi) \\ N_r &= \frac{1}{4}(1 + 3 \cos 2\psi) \\ N_\psi &= -\frac{3}{4} \sin 2\psi \end{aligned} \quad (\text{B8})$$

Remembering that the characteristic MONDian bubble size, denoted r_0 , is given by the expression

$$r_0 = \left(\frac{4\pi}{\kappa}\right)^2 \frac{a_0}{A} \quad (\text{B9})$$

Such that we can write

$$w = \frac{\kappa^2}{16\pi^2} \frac{|\nabla \Phi_N|}{a_0} = \frac{r}{r_0} N \quad (\text{B10})$$

giving us the form of the source term

$$\nabla^2 \phi = \frac{4\pi a_0 / \kappa}{\sqrt{4r r_0}} \left(\frac{N_r}{N^{1/2}} + \frac{N_\psi}{N^{3/2}} \frac{\partial N}{\partial \psi} \right) \left(1 + \left(\frac{rN}{r_0} \right)^2 \right)^{-3/4} \quad (\text{B11})$$

The problem here is akin to electrostatics, solving the equations subject to the boundary conditions that $\delta \mathbf{F}_\psi$ vanishes (and $\delta \mathbf{F}_r$ equate) at $\psi = 0$ and π , such that we avoid a jump in the field at $\psi = \pi/2$.

a. DM Regime

For $r \ll r_0$, it's clear Equation (B11) reduces to:

$$\nabla^2 \phi = \frac{4\pi a_0 / \kappa}{\sqrt{4r N r_0}} \left(N_r + \frac{N_\psi}{N} \frac{\partial N}{\partial \psi} \right) \left\{ 1 - \frac{3}{4} w^2 + \dots \right\} \quad (\text{B12})$$

where the angular functions of the leading order term neatly reduce to

$$\frac{7 + 9 \cos 2\psi}{(2(5 + 3 \cos 2\psi))^{5/4}} = g(\psi) \quad (\text{B13})$$

The separable form of the source suggests an ansatz of

$$\phi = C_1 r^a F(\psi) \quad (\text{B14})$$

where C_1 is a constant, the exact form of which is fixed from the source term. This gives rise to a sourced second order ODE:

$$r^{a-2} (a(a+1)F + \cot(\psi) F' + F'') = r^{-1/2} g(\psi) \quad (\text{B15})$$

where $' = \partial/\partial\psi$ and

$$C_1 = \frac{4\pi a_0}{\kappa \sqrt{r_0}} \quad (\text{B16})$$

We find that the solutions of the homogenous equation are Legendre Polynomials of order a , with the form of (B15) suggesting $a = 3/2$ and the inhomogeneous solution is found to be

$$F \approx -0.0236 - 0.1886 \cos 2\psi + 0.0108 \cos 4\psi \quad (\text{B17})$$

We can then compute the components of the MONDian force

$$\begin{aligned} -\nabla \phi &= \frac{4\pi a_0}{\kappa} \left(\frac{r}{r_0} \right)^{0.5} (F_r \mathbf{e}_r + F_\psi \mathbf{e}_\psi) \\ F_r &\approx 0.0354 + 0.2829 \cos 2\psi - 0.0162 \cos 4\psi \\ F_\psi &\approx -0.3772 \sin 2\psi - 0.0432 \sin 4\psi \end{aligned} \quad (\text{B18})$$

and we compare angular profile functions for type I and IIB solutions in Figure 6. We see from the form of the MONDian force,

$$\delta \mathbf{F} = -\nabla \phi = \frac{4\pi a_0}{\kappa} \left(\frac{r}{r_0} \right)^p \mathbf{S}(\psi) \Rightarrow S_{ij} \propto r^{p-1}$$

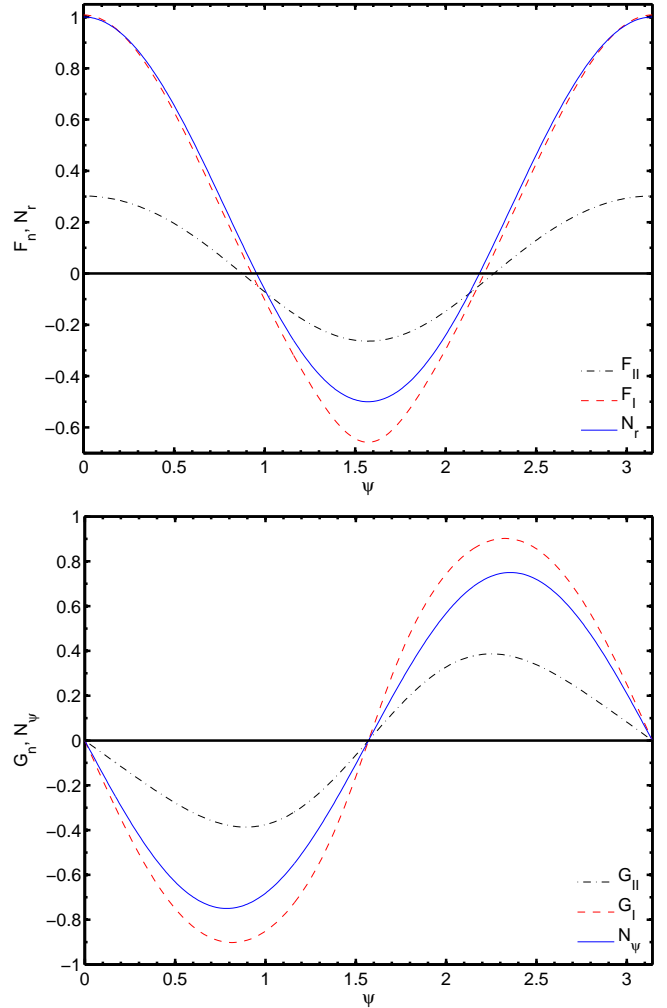


FIG. 6: The angular profile functions F and G for the inner bubble forces in both type I and type IIB theories, alongside the linear Newtonian radial and azimuthal angular profiles.

where in type I, $p \simeq 0.764$ and in type IIB, $p = 0.5$ - clearly the tidal stresses will have a sharper divergence as we approach the SP. This is due to the modified Poisson equation being linear in ϕ and so with no curl forces present, the inner bubble solutions are not softened as they are in a non-linear theory.

In addition, at the saddle we have region where $|\mathbf{g}_N| = 0$ and so we need to consider solutions to the Laplace equation

$$\nabla^2 \phi_L = 0 \quad (\text{B19})$$

which subject to smoothness and continuity conditions being satisfied and regularity at the origin, can be written in general by

$$\phi_L = \frac{4\pi a_0}{\kappa} \sum_{\ell} A_{\ell} r^{\ell} P_{2\ell}(\cos \psi) \quad (\text{B20})$$

where $P_{2\ell}(\cos \psi)$ are Legendre polynomials,

$$A_\ell = \frac{a_\ell}{r_0^{\ell-1}} \quad (\text{B21})$$

and a_ℓ are dimensionless constants to be found by matching solutions at the intermediate MONDian regime (akin to the DM scaling C in type I theories). Our normalisation is picked such that $\nabla\phi$ has units of acceleration. We only need to expand out a few terms from this contribution, since the region of validity of these solutions is small.

b. QN Regime

For $r \gg r_0$, we find (B11) reduces to:

$$\nabla^2 \phi = \frac{4\pi a_0}{\kappa} \frac{r_0}{2r^2 N^2} \left(N_r + \frac{\partial N}{\partial \psi} \frac{N_\psi}{N} \right) \left\{ 1 - \frac{3}{4} \frac{1}{w^2} + \dots \right\} \quad (\text{B22})$$

where at leading order, we label the source term

$$\frac{2(7 + 9 \cos 2\psi)}{(5 + 3 \cos 2\psi)^2} = h(\psi) \quad (\text{B23})$$

In order to satisfy our boundary conditions, our ansatz for the leading term needs to be of the form

$$\phi_2 = C_1 H_2(\psi) + C_2 \ln \left(\frac{r}{r_0} \right) \quad (\text{B24})$$

Computing the Laplacian gives

$$\nabla^2 \phi = \frac{C_1}{r^2} \frac{1}{\sin \psi} \frac{\partial}{\partial \psi} (\sin H_2') + \frac{C_2}{r^2} r_0 = \frac{4\pi a_0 r_0}{\kappa} \frac{h(\psi)}{r^2} \quad (\text{B25})$$

allowing us to set

$$C_1 = C_2 r_0 = \frac{4\pi a_0 r_0}{\kappa} \quad (\text{B26})$$

Integrating out once then gives

$$\sin \psi \frac{\partial H_2}{\partial \psi} = \int (h - 1) \sin \psi d\psi + A \quad (\text{B27})$$

and from the boundary conditions, we find

$$A = - \left(\frac{3}{2} + \frac{\pi}{3\sqrt{3}} \right) \quad (\text{B28})$$

meaning we solve (B27) to find

$$H_2 \approx -0.2292 + 0.2876 \cos 2\psi - 0.1163 \cos 4\psi \quad (\text{B29})$$

Expanding to higher terms will result in the series

$$\phi = \phi_2 + \frac{4\pi}{k} a_0 \sum_{n=2}^{\infty} C_n \left(\frac{r}{r_0} \right)^{2-2n} H_n(\psi) + \frac{\kappa}{4\pi} \Phi_N \quad (\text{B30})$$

where $H_n(\psi)$ satisfies the sourced ODE

$$n(n+1)H_n + \cot(\psi)H_n' + H_n'' = h_n \quad (\text{B31})$$

and h_n is given by

$$h_n(\psi) = \frac{2^{3n/2-2}(7 + 9 \cos 2\psi)}{(5 + 3 \cos 2\psi)^{n/2+1}} \quad (\text{B32})$$

We also always have the background rescaled Newtonian contribution

$$\frac{\kappa}{4\pi} \Phi_N = -\frac{\kappa}{4\pi} \frac{Ar^2 Nr}{2} = -\frac{4\pi a_0}{\kappa} \frac{r^2}{8r_0} (1 + 3 \cos 2\psi) \quad (\text{B33})$$

which obviously is the dominant contribution in the $r/r_0 \gg 1$ limit.

Appendix C: Adaptations to the Numerical Code

The main dynamics of the relaxation code used are outlined in Appendix A of [4] and here we detail how it can be adapted to solve the type II Poisson equation. First we must frame (2) in the form of

$$\nabla \cdot \mathbf{g} = \frac{k}{4\pi} \nabla \cdot (\nu \mathbf{g}_N) \quad (\text{C1})$$

$$\nabla \wedge \mathbf{g} = 0 \quad (\text{C2})$$

next compute the discrete divergence

$$D_{\mathbf{x}} = \sum_j \frac{g_{\mathbf{x}}^j - g_{\mathbf{x}-\mathbf{j}}^j}{\Delta_-^j} \quad (\text{C3})$$

where we use the compact notation

$$\Delta_-^j = r_{\mathbf{x}}^j - r_{\mathbf{x}-\mathbf{j}}^j$$

$$\Delta_+^j = r_{\mathbf{x}+\mathbf{j}}^j - r_{\mathbf{x}}^j$$

Finally the source term takes the form

$$D_{\mathbf{x}}^N = \sum_j \frac{\nu_{\mathbf{x}}(g_{\mathbf{x}}^j)_N - \nu_{\mathbf{x}-\mathbf{j}}(g_{\mathbf{x}-\mathbf{j}}^j)_N}{\Delta_-^j} \quad (\text{C4})$$

such that at each site we locally solve (C1) whilst ensuring the discrete curl (C2) is satisfied globally. As the field changes $g^j \rightarrow g^j + \delta g^j$, then at each step, these changes should take the form

$$\delta g_{\mathbf{x}}^j = + \frac{C_{\mathbf{x}}}{\Delta_+^j}$$

$$\delta g_{\mathbf{x}-\mathbf{j}}^j = - \frac{C_{\mathbf{x}}}{\Delta_-^j} \quad (\text{C5})$$

to keep the discrete curl satisfied. The change in the discrete divergence, $\delta D_{\mathbf{x}}$, at each step will satisfy,

$$D_{\mathbf{x}} + \delta D_{\mathbf{x}} = D_{\mathbf{x}}^N \quad (\text{C6})$$

such at each site, the change in the field is given by

$$\delta g_{\mathbf{x}}^j = -\frac{D_{\mathbf{x}} - D_{\mathbf{x}}^N}{\delta D_{\mathbf{x}}} \frac{C_{\mathbf{x}}}{\Delta_+^j} \quad (\text{C7})$$

Then as we cycle through the lattice and the \mathbf{g} field converges, the additional changes to $g_{\mathbf{x}}^j$ lessen. We achieve faster convergence using a successive over relaxation method (SOR), by scaling the field as

$$\delta g_{\mathbf{x}}^j \rightarrow \lambda \delta g_{\mathbf{x}}^j \quad (\text{C8})$$

where λ is the over-relaxation parameter and is larger than unity. We begin with $\lambda = 1$ and increase it once the field is settling down, since high values of λ can initially result in the RMS value of $|\delta D_{\mathbf{x}}|$ increasing, whilst we are looking for $|\delta D_{\mathbf{x}}| \rightarrow 0$.

-
- [1] M. Milgrom, *Astrophys. J.* **270**, 365 (1983).
[2] B. Famaey and S. S. McGaugh, *Living Reviews in Relativity* **15**, 10 (2012), 1112.3960.
[3] J. Bekenstein and J. Magueijo, *Phys. Rev.* **D73**, 103513 (2006), astro-ph/0602266.
[4] N. Bevis, J. Magueijo, C. Trenkel, and S. Kemble, *Class. Quant. Grav.* **27**, 215014 (2010), 0912.0710.
[5] J. Magueijo and A. Mozaffari, *Phys. Rev. D* **85**, 043527 (2012), 1107.1075.
[6] P. McNamara, S. Vitale, and K. Danzmann (LISA), *Class. Quant. Grav.* **25**, 114034 (2008).
[7] C. Trenkel, S. Kemble, N. Bevis, and J. Magueijo, submitted (2009).
[8] A. Mozaffari, *Phys. Rev. D* **87**, 064034 (2013), 1212.3905.
[9] P. Galianni, M. Feix, H. Zhao, and K. Horne, *Phys. Rev. D* **86**, 044002 (2012), 1111.6681.
[10] J. Bekenstein and M. Milgrom, *Astrophys. J.* **286**, 7 (1984).
[11] M. Milgrom, *Phys. Rev.* **D80**, 123536 (2009), 0912.0790.
[12] T. Clifton and T. G. Zlosnik, *Phys. Rev. D* **81**, 103525 (2010), 1002.1448.
[13] B. S. Sathyaprakash and B. F. Schutz, *Living Rev. Rel.* **12**, 2 (2009), 0903.0338.
[14] F. Antonucci and M. A. et al, *Classical and Quantum Gravity* **28**, 094001 (2011), URL <http://stacks.iop.org/0264-9381/28/i=9/a=094001>.
[15] H.-S. Zhao and B. Famaey, *Astrophys. J.* **638**, L9 (2006), astro-ph/0512425.
[16] T. G. Zlosnik, P. G. Ferreira, and G. D. Starkman, *Phys. Rev. D* **74**, 044037 (2006), gr-qc/0606039, URL <http://adsabs.harvard.edu/abs/2006PhRvD...74d4037Z>.
[17] J. D. Bekenstein, *Phys. Rev.* **D70**, 083509 (2004); Erratum-ibid. **D71**, 069901 (2005), astro-ph/0403694.
[18] T. Clifton, P. G. Ferreira, A. Padilla, and C. Skordis, *Physics Reports* **513**, 1 (2012).
[19] S. M. Carroll and E. A. Lim, *Phys. Rev. D* **70**, 123525 (2004), hep-th/0407149.
[20] K.-i. Umezu, K. Ichiki, and M. Yahiro, *Phys. Rev. D* **72**, 044010 (2005), astro-ph/0503578v1.